

## THE STEADY-STATE PROPERTY 'FORCE-DEFORMATION' FOR PASSIVE MYOCARDIUM

Yu.L. Protsenko\*, A.V. Kobelev\*\*, R.M. Kobeleva\*, S.M. Routkevich\*

\* Ekaterinburg branch of the RAS Institute for Ecology and Microorganism Genetics, 620219, Pervomayskaya 91, Ekaterinburg, Russia

\*\* Institute for Metal Physics UrD of RAS, Kovalevskoy 18, Ekaterinburg, Russia, e-mail: kobelev@imp.uran.ru

**Abstract.** The elastic properties of heart muscle preparation are studied in the stationary state in the isometric regime at low simulation frequency, between contractile excitations. The measurements of stress and transversal size as the functions of the sample length were conducted on a papillary muscle of rabbit by the method described previously. The non-linearity of 'stress-strain' dependencies was revealed, which manifests itself in the increase of stiffness at loading. The relation of cross-section size and the length of myocardium preparation were also ascertained. The mathematical description was presented in the framework of 2D structure dependent functional rheological model of inhomogeneous myocardium. The model consists of linear elastic Hooke's elements, and describes these non-linear properties due to variations in geometry with deformation. Nine types of such models with different topology were considered and corresponding stress-strain curves were obtained for all of them. The sizes and elastic modules of constituent Hooke's elements for two of the models with best-fit characteristics were estimated by comparison with experimental data.

**Key words:** myocardium biomechanics, stress-strain curves, nonlinear mechanical properties

### Introduction

The relation between the force and the length (or 'pressure-volume' relation), measured both in systole and diastole in the physiological range of deformations ( $\varepsilon \leq 0.3$ ), is the determining feature in studying contractility of myocardium [1]. The primary protein elements of muscle tissue structure such as myosin, actin and titin filaments in sarcomers, collagen fibers in the frame of connective tissue, can be treated mechanically, accurately enough, as Hooke's elements in which passive force linearly depends on extension [2, 3]. The morphological structure of both cardiomyocytes and its environment connective frame is a lattice with rather sophisticated topology [4]. This is possibly the reason for elastic non-linearity of isolated myocardium tissue and a heart in total.

At present it is lack of the functional rheological model that describes experimental stress-strain data in the whole range of deformations. The existing models are simply the 1D combinations of elastic and viscous elements [3], or at least are processed in trivial linear range for determining elastic module [5].

### The aim of the study

The aim of the study focuses on the development of 2D topological structure to describe passive force-length dependencies for myocardium. The primary Hooke's elements are specified by their lengths and elasticity coefficients. The non-linearity of the model is due to its geometry. On the base of the comparison of these results with experimental dependencies the conclusion on sufficiency of that or another model can be made. The lengths of primary elements and corresponding elastic modules should be estimated. The purpose is to determine the ranges of parameters values in which the non-linear effect is most pronounced.

### Experiment

#### Method

The choice of experimental method was conditioned by the fact that the mechanical trial by uniaxial loading of separate preparation of the heart chamber wall or the heart in total cannot give reliable values of visco-elastic properties. This is caused by random variations of the directions of filaments in the muscle, and hence, by the anisotropy of the properties. We carry out experiments on isolated samples of the papillary muscle that allow avoiding difficulties due to identical directions of filaments in the preparation. Special attention is undertaken to consider the damage of the preparation ends at fixing.

The measurements of dimensions were carried out with the help of the optical markers in the central segment of the preparation by the binocular microscope with built-in TV camera. Micro-strain were assigned with linear servomotor and controlled by PC software. Corresponding stress values were measured by strain gages. The protocol of the trial was registered and stored as the numerical computer files. The measurement procedure is described in detail in [6].

#### Preparations

Three types of myocardium samples were chosen, which differ in the physiological stiffness degree  $P_{act} / P_{pas}$ , which means the ratio of passive state stress and maximum active stress in isometric regime at the same length. The preparation is called 'soft' if this ratio is smaller than 0.3. It proves indirectly the absence of contractile places in the preparation. The initial parameters of the samples are presented in Table 1.

Experimental data on samples 2 and 3 are obtained at optical markers on different sides of the same preparation.

Table 1. The original parameters of the samples.

Sample	1	2	3	4
Designation	MF1-L <sup>2</sup>	MW1-L	MW2-L	AZ0-L
$P_{pas} / P_{act}$	2.49	0.77	0.67	0.22
$h$ , mm	0.9	0.7	0.7	0.7
$l_0$ , mm	3.25	6.5	6.5	3.5
$l_{max}$ , mm	3.94	7.37	7.37	4.72
$K_{sta}$ , G/mm ( $E_{sta}$ , G/mm <sup>2</sup> )	0.48 (2.45)	0.21 (3.55)	0.19 (3.2)	0.1 (0.9)
$K_{fin}$ , G/mm ( $E_{fin}$ , G/mm <sup>2</sup> )	1.78 (9.09)	3.03 (51.2)	2.64 (44.6)	0.64 (5.8)

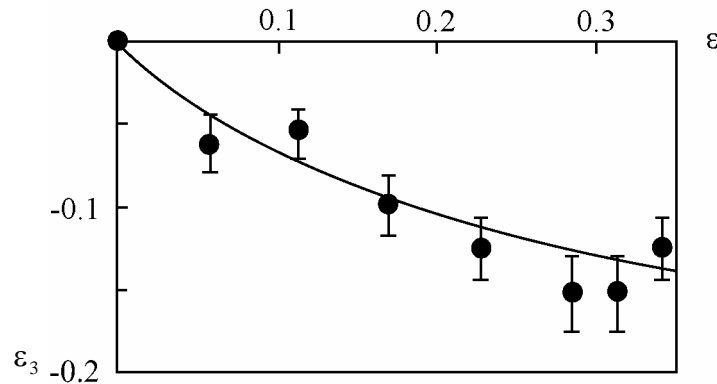


Fig. 1. Experimental dependence of transversal deformation on longitudinal for the sample of rabbit papillary muscle.

#### Transversal – longitudinal deformation dependence

The decreasing the sample cross-section takes place as a rule at longitudinal stretching, that is characterized by Poisson ratio  $\sigma_p = -\varepsilon_3 / \varepsilon$ , where  $\varepsilon_3$  is the transversal strain. Fig. 1 presents experimental dependence, which, as a whole, is non-linear with plateau at the end of the curve.

#### Stationary stress-strain dependence

Experimental data on all of the samples demonstrate non-linear character of stationary stress dependence on the sample length in the physiological range of strain. The initial part of the stress-strain curve is specified by small ‘local’ stiffness  $K_{sta}$ , whereas the values of ‘local’ stiffness rise with the increase of deformation ( $K_{fin}$ ). Table 1 presents the values of local elastic modules  $E_{sta}$  and  $E_{fin}$ , which relate to the stiffness coefficients by  $E = Kl / S$ , where  $l$  is preparation length and  $S$  is its cross-section area.

### Modeling of ‘force-deformation’ property

#### Assumptions

Neglecting viscosity, it is assumed that the morphological variety of myocardium tissue structures can be deduced from three types of primary linear elements. Let  $l_1, l_2, l_3$  be the lengths of these elements, and  $K_1, K_2, K_3$  be the corresponding stiffness coefficients. The 2D topologically different models, which have functionally individual elastic properties, can be deduced by combination of these three elements with frictionless joints. Each of the elements may be longitudinal, transversal, inclined, or cross-connected. Note that all these models should have the center of symmetry that helps to avoid difficulties arising with distortion. In accordance with experimental conditions, the stress-strain curves are measured on a separate muscle sample with fixed ends. So we assume that the applied stretching force is distributed over the definite area of rigid bar of diameter  $h$ , to the edges of which the primary elements are connected. For the sake of simplicity of calculations, some of the models assume  $h \rightarrow 0$ .

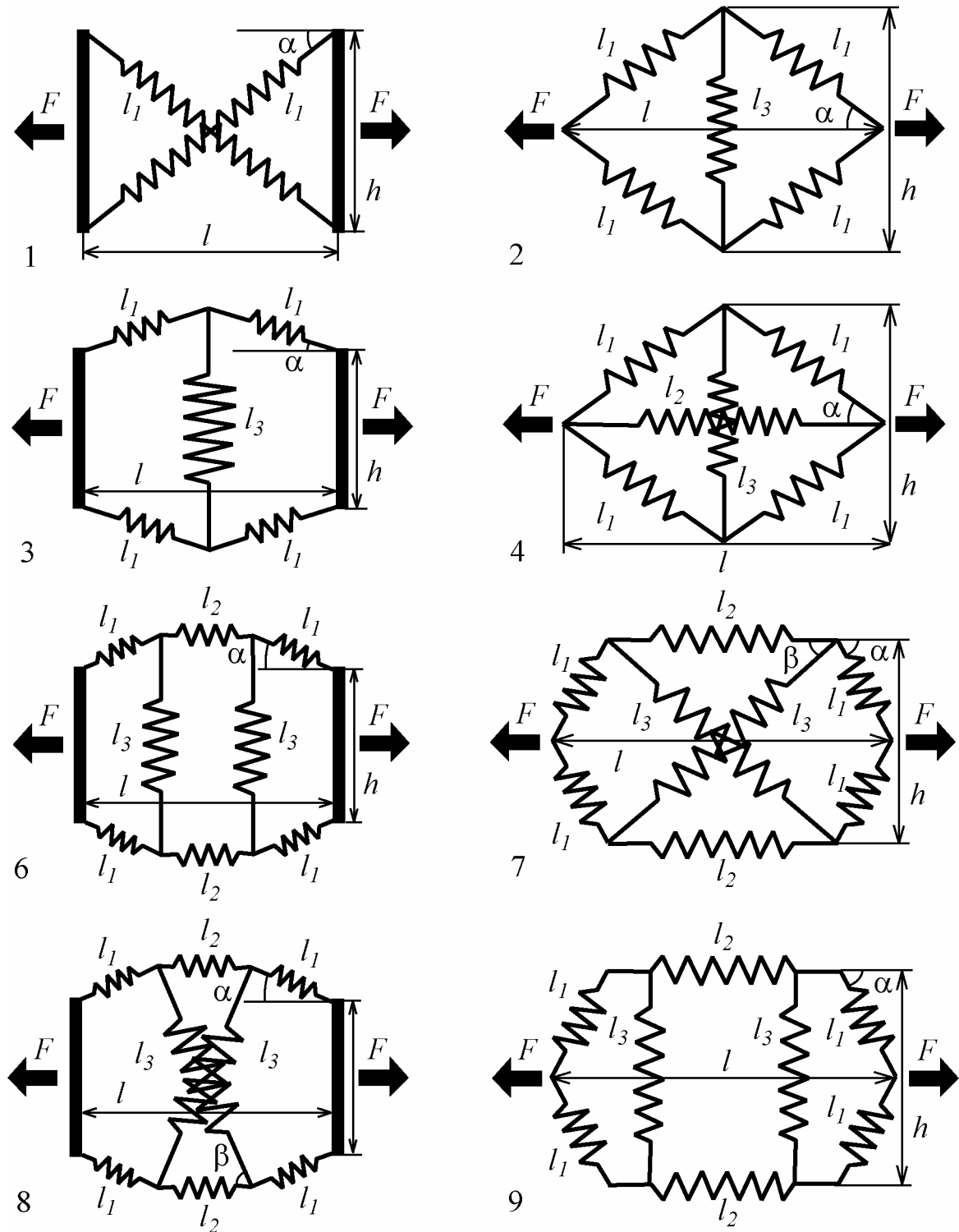


Fig. 2. 2D models of topological structures assembled from Hooke's elements presented by springs and connected with frictionless joints (models (1-9)).

### Model structure

Nine topologically different kinds of such models are considered and corresponding graphs are depicted in Fig. 2. Obvious generalization to 3D case, more close to real objects, is given by the figures obtained by rotation of these structures around the longitudinal axis. Despite the linearity of primary Hooke's elements in which the force is a linear function of stretching, it is obvious that the structure as a whole may be non-linear due to its geometry.

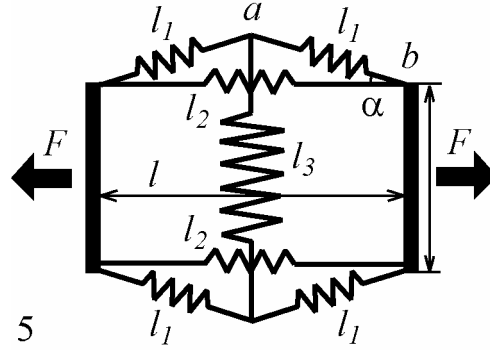


Fig. 3. Block design of model 5, consisting of three types of elements (inclined  $l_1$ , longitudinal  $l_2$  and transversal  $l_3$ ) connected in the points  $a$  and  $b$  with each other and with rigid bar  $h$ .

Model 1 with cross-connected elements possesses ‘trigonometric’ non-linearity. Models 7 and 8 also have cross-connected elements. Models 2 and 4 differ in longitudinal element giving additive contribution. The same is true for the models 3 and 5, despite the fact that longitudinal element contribution is not additive. It is obvious, that there are the limits at  $h \rightarrow 0$  from the models 6 and 8 to the models 7 and 9 and from the models 3 and 5 to the models 2 and 4. Besides, model 6 at the elimination of the longitudinal element ( $l_2 \rightarrow 0$ ) converse to 3 and 8 to 2.

Note that the transversal dimension in the center of 2D structure of the models 3, 6 and 8 may be either greater or smaller than  $h$ , that does not change the topology of the model and result in computational formulae. In this case the longitudinal stretching results in  $l_3$  increase, so that analog of Poisson ratio  $\sigma_p$  becomes negative.

So we consider consequently 13 models, with 4 of them topologically equivalent to others. In every, but one, of the models the explicit exact expressions for the force as a function of deformations of all elements and dependencies of strain on each other were derived. In one case not-explicit solution was found.

#### Initial equations and calculation formulae

Let us present the sketch of the calculations, for instance, of model 5 (Fig. 3). The set of the equations for relative strain of the elements  $\varepsilon_1$ ,  $\varepsilon_2$ ,  $\varepsilon_3$  can be deduced from the equilibrium conditions at the points  $a$  and  $b$  in the axes projection:

$$\begin{aligned} \varepsilon_1 \cos \alpha &= \kappa_1, \\ \varepsilon_2 &= f, \\ \kappa_3 \varepsilon_1 \sin \alpha + \kappa_1 \varepsilon_3 &= 0. \end{aligned} \quad (1)$$

Here we use the following notations:

$$\begin{aligned} l_1 &= l_{01}(l + \varepsilon_1), \quad l_2 = l_{02}(l + \varepsilon_2), \quad l_3 = l_{03}(l + \varepsilon_3), \\ k_1 &= K_1 l_{01}, \quad k_2 = K_2 l_{02}, \quad k_3 = K_3 l_{03}, \\ f &= \frac{F}{k_2}, \quad \kappa_1 = \frac{k_2}{k_1}, \quad \kappa_3 = \frac{k_2}{k_3}. \end{aligned} \quad (2)$$

In the considered model the length and strain of longitudinal element coincide with the total length and strain, respectively  $l_0 = l_{02}$ ,  $\varepsilon = \varepsilon_2$ . It is convenient to assign initially transversal strain  $\varepsilon_3$  in the range  $(0, \varepsilon_{3\max})$  and to find solution as the function of  $\varepsilon_3$ . This results in:

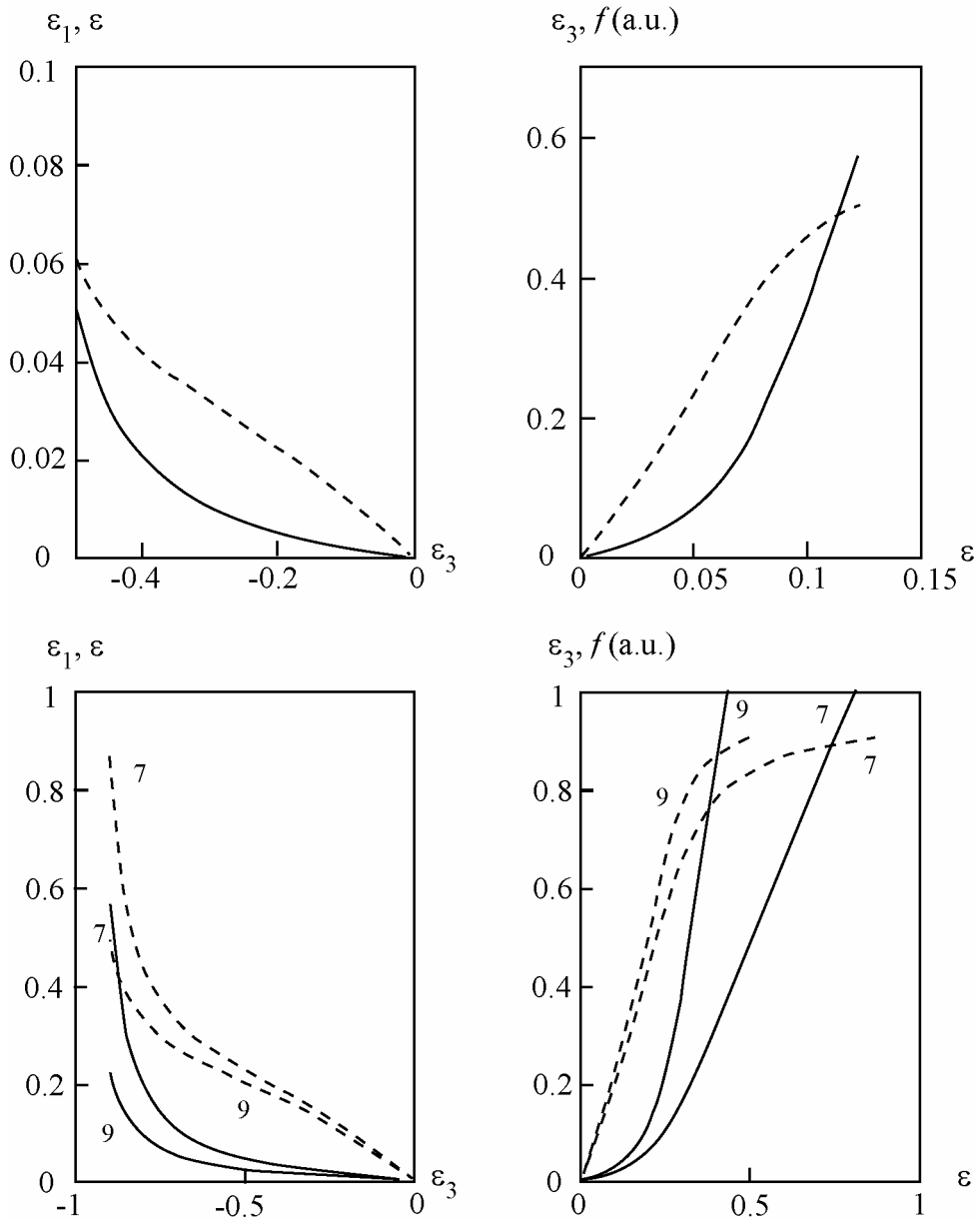


Fig. 4. Inclined element strain  $\varepsilon_1$  (solid line) and total longitudinal deformation (dashed line)  $\varepsilon$  as the functions of transversal deformation  $\varepsilon_3$  (left panel). Right panel depicts transversal deformation (dashed line) and force in arbitrary units (solid line) dependences on longitudinal deformation. In the bottom the same is shown for the models designated according to Fig. 2.

$$\begin{aligned}
 \varepsilon_1(\varepsilon_3) &= -\frac{\kappa_1 \lambda_1 \varepsilon_3}{2\kappa_3(y_3(\varepsilon_3) - \gamma) + \kappa_1 \lambda_1 \varepsilon_3}, \\
 \varepsilon(\varepsilon_3) &= -1 + \sqrt{y_1^2(\varepsilon_3) - (y_3(\varepsilon_3) - \gamma)^2}, \\
 f(\varepsilon_3) &= -\frac{\varepsilon_3 + [\varepsilon_3 - \kappa_3(y_3(\varepsilon_3) - \gamma)]\varepsilon(\varepsilon_3)}{\kappa_3(y_3(\varepsilon_3) - \gamma)},
 \end{aligned}
 \tag{3}$$

where

$$\begin{aligned}
 y_1(\varepsilon_3) &= \lambda_1(l + \varepsilon_1(\varepsilon_3)), & y_3(\varepsilon_3) &= \lambda_3(l + \varepsilon_3), \\
 \lambda_1 &= \frac{l_{01}}{l_0}, & \lambda_3 &= \frac{2l_{03}}{l_0}, & \gamma &= \frac{h}{l_0}.
 \end{aligned}
 \tag{4}$$

#### Basic dependencies

The dependencies of strain of longitudinal and inclined elements on transversal strain show their non-linear character (see Fig. 4, cf. Fig. 1). The dependencies  $\varepsilon_1(\varepsilon_3)$ ,  $\varepsilon(\varepsilon_3)$  (left panel) are obtained in the assumption that inclined elements stiffness coefficient is two orders greater than for longitudinal and transversal ones. The saturation of the total strain is reflected in the non-monotone dependence (curve  $\varepsilon(\varepsilon_3)$ ). The  $f(\varepsilon_3)$  dependence (Fig. 4, right panel) corresponds to two asymptotic regimes of strain and presents the ‘stiffness amplification’ effect, that means the increase of stiffness with strain, which is explained by ‘trigonometric’ non-linearity, and on the other hand, by ‘collapse’ effect when inclined elements gain longitudinal direction. The latter effect results in the fact that the ‘soft’ element works at small strain, while the ‘rigid’ element works at large strain after collapse occurs. Similar behavior has been found for all of the models investigated with definite relation between parameters. Fig. 4 (bottom) presents examples of corresponding plots for some other models.

#### Comparison with experiment

The shape of the stress-strain curve may be controlled by three groups of parameters. The values of transversal and cross-connected elements’ stiffness parameters are responsible for the slope of the initial part of stress-strain curve. The relation between geometric parameters is responsible for the position of the point where one regime is changed by another. And at last, stiffness parameter of inclined element determines the slope of the final part of the curve. Besides, the comparison of the results from various models shows that they are sensitive in different ways to the changes in parameters values; it will be demonstrated on the data of one experiment.

We choose the data of experiment 3 as the reference experimental data according to which elastic properties of various models should be analyzed. Fig. 5 (left panel) presents stress-strain curves obtained in the models in which there are cross-connected (1), parallel longitudinal and inclined elements (6) and (9) and their combinations (7). All these models cannot give reliable description of experimental data (rectangles) despite optimization of fitting parameters. The models with more close description of the features of experimental dependencies are presented in the left panel. Those are mainly the models of "rhombic" geometry (if we neglect the parameter  $h$  is finite) in which inclined and transversal elements are determining ones.

Further, we shall take models 3 and 5 which differ each other inessentially in the topology (by the presence of longitudinal element) and functionally for processing of experimental data. These models, in our opinion, are most suitable for the description of various experimental curves due to their "flexibility" and sensitivity to parameters changes.

The main geometric parameters of the models, such as  $l_3$ , the length of transversal element,  $l_1$ , the length of inclined element, and corresponding strain are presented in Table 2. The cross-sectional size  $h$  and the total longitudinal length  $l$  are assumed to coincide with experimental data (see Table 1). Note that despite low maximum longitudinal

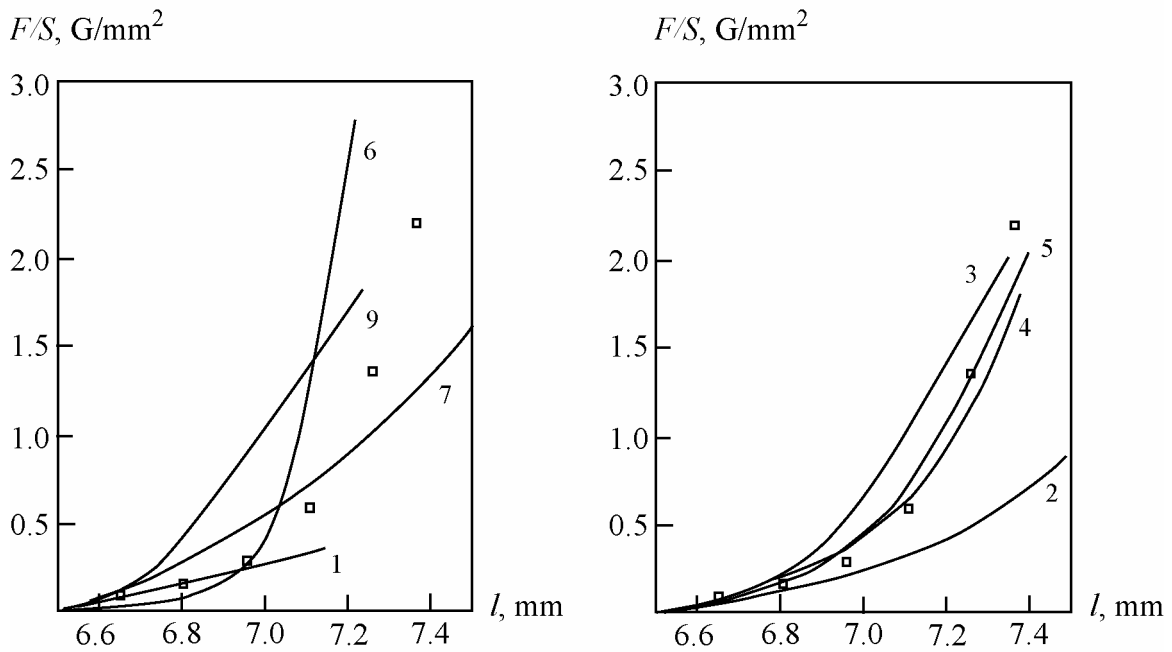


Fig. 5. 'Force-length' curves for the models designated according to Fig. 2 in comparison with experimental data on sample 3.

Table 2. Values of parameters for two models obtained by processing of experimental data

Samples	1		2		3		4	
Models	3	5	3	5	3	5	3	5
$l_3$ , mm	2.4	2.4	3.8	3.8	3.4	3.4	4.0	3.7
$\varepsilon_{3\max}$	-0.33	-0.48	-0.65	-0.7	-0.65	-0.68	-0.45	-0.55
$\varepsilon_{\max}$	0.221	0.244	0.137	0.138	0.145	0.135	0.357	0.363
$l_1$ , mm	1.79	1.79	3.6	3.6	3.52	3.52	2.4	2.3
$K_1$ , G/mm	2	1.6	4.1	4.3	2.4	2.5	2.1	1.2
$K_2$ , G/mm	–	0.4	–	0.06	–	0.06	–	0.04
$K_3$ , G/mm	0.2	0.05	0.03	0.02	0.03	0.02	0.06	0.03
$E_1$ , G/mm <sup>2</sup>	140	110	145	152	87	90	110	66
$E_2$ , G/mm <sup>2</sup>	–	16	–	1.2	–	1.2	–	1.4
$E_3$ , G/mm <sup>2</sup>	11	2.7	1	0.7	1.1	0.7	1.9	1

strain  $\varepsilon_{\max}$  is within the range of physiological limits, the transversal strain  $\varepsilon_{3\max}$  is rather high.

General agreement between the theoretical curves and experimental data is pretty good, as can be seen (Fig. 6) for the both models 5 and 3 with slight advantage for the first. The range of initial length values, total strain and differences in the slope of the curves is rather great to make the conclusion that the models are adequate. The values of all parameters obtained by fitting procedure are reliable in the sense of sensitivity of the curve to the last digit changing.

Note that the values of stiffness parameters ( $K_1$ ,  $K_2$ ,  $K_3$ ) of the primary elements differ in more than the order of magnitude. The corresponding values of Young's modules

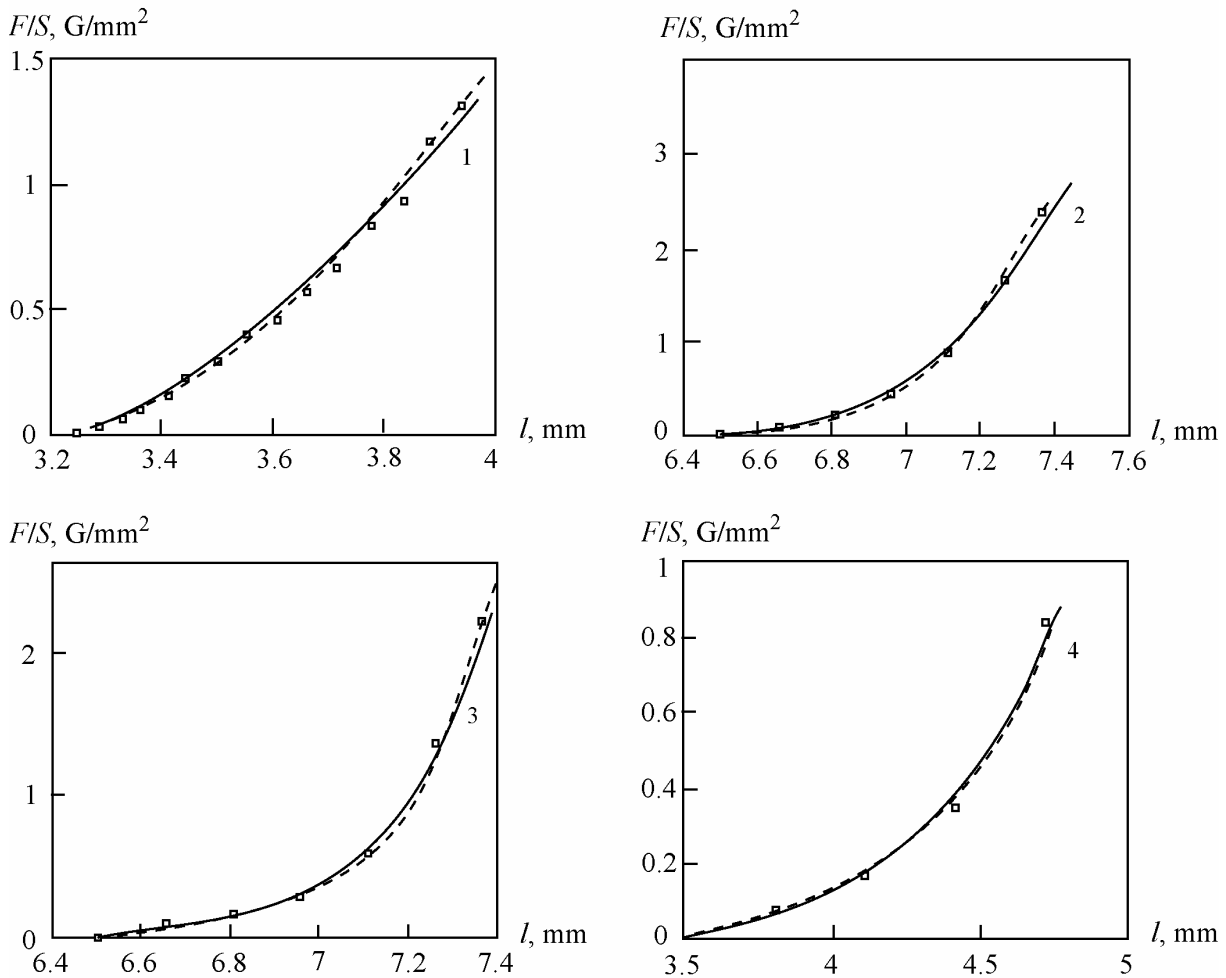


Fig. 6. The best-fit results for the models 3 (dashed line) and 5 (solid line) and experimental data 1-4.

( $E_1$ ,  $E_2$ ,  $E_3$ ) are calculated in the assumption that the transversal size of an element is 1/10 of its initial length.

### Discussion

The passive state elastic ‘stress-strain’ properties in the physiological range of strain and the effect of rigidity increase with strain have high enough degree of generality for all soft living tissues, and particularly for the myocardium. Our approach to the modeling of this effect demonstrate that geometric factor can play significant role in its understanding.

The values of ‘soft’ and ‘rigid’ elements elastic modules determined by the experimental data and the theoretical model dependencies fitting procedure do not coincide with the values of ‘local’ elastic modules obtained from the slope of experimental ‘stress-strain’ curve. The latter depend on the model geometry. Quite good agreement exists between the ranges of results obtained and tabular data of elastic modules values of some materials (the rubber  $E = 150 G/mm^2$ , the elastine  $E = 60 G/mm^2$ ) and other investigators’ data ([5]  $K = 8.7 G/mm$  for the transversal stiffness coefficient at biaxial stretching of dog’s heart wall). This allows us to make identification of the primary elements material with the proteins of the myocardium connective tissue.

The sizes of transversal (and cross-connected) elements, which are to be used in one or another model for successful comparison of the theory and the experiment, appear to be not much smaller than the total length of the sample. This is true for the real preparations, e.g. the ratio of cross-section length and total length for the preparation, the data for which are presented in Fig. 1, is 0.3 at the initial conditions. The transversal strain, however, in the models describing satisfactorily experimental data is in most cases greater than the longitudinal one, especially at the initial stages. This indicates that one cannot assume the investigated objects in terms of solid state ( $\sigma_p$  may become greater than unity) and also underlines the role of inhomogeneity, i.e. the difference of the elastic properties of constituent elements at various cross-sections. It is clear, in this connection, that 3D modeling which use spiral-wise elements allows one to avoid these difficulties.

Recently numerous communications report that the intercell albumin titin makes the basic contribution to generation of the myocardium stress in passive state [7]. In our approach the inclined and longitudinal elements ( $l_1$  and  $l_2$ ) can be treated as the model of titin as the joint albumin. Especially as it was shown that titin domains could be assumed as Hooke's elements [8]. The alternative investigations [9,10] are based on the assumption that "stress-strain" dependence at separate filaments level is nonlinear. The morphological data are absent, and it is quite natural to believe that it is lack of sequentially linked chains of cardiomyocytes by the end-walls in the preparations of separated myocardium. Moreover, one cannot exclude in this case the contribution of the skeleton of myocardium connective tissue into generation of passive stress, because they play the role of a frame, although they are numbered by 1/5 of all elements.

### References

1. ИЗАКОВ В.Я., ИТКИН Г.П., МАРХАСИН В.С., ШТЕНГОЛЬД Е.Ш., ШУМАКОВ В.И., ЯСНИКОВ Г.П. **Биомеханика сердечной мышцы**. М., Наука, 1981 (in Russian).
2. ИЗАКОВ В.Я., МАРХАСИН В.С., ЯСНИКОВ Г.П., БЕЛОУСОВ В.С., ПРОЦЕНКО Ю.Л. **Введение в биомеханику пассивного миокарда**. М., Наука, 2000 (in Russian).
3. TROMBITAS K., REDKAR A., CENTER TH., WU Y., LABEIT S., GRANZIER H. Extensibility of isoform of cardiac titin: variation in contour length of molecular subsegments provides a basis for cellular passive stiffness diversity. **Biophysical J**, 79(12): 3226-3234, 2000.
4. ROBINSON TH.F., GERASI M.A., SONNENBLICK E.H., FACTOR ST. M. Coiled permyisial fibers of papillary muscle in rat heart: morphology, distributions and changes in configuration. **Circ Res**, 63(3): 577-592, 1988.
5. HALPERIN H.R., CHEW P.H., TSITLIC J.E., et. al. Regional myocardium wall stress, ch. 9. In: Sideman S., Beyar R. (Editors). **Simulation and control of cardiac system**, V. I, CRC Press, Boca Raton, Florida, 113-121, 1987.
6. ПРОЦЕНКО Ю.Л., РУТКЕВИЧ С.М., ЗОЛУТУШНИКОВ В.В., АБАЗОВ В.А. Метод экспериментального исследования реологических характеристик препарата миокарда. **Российский физиологический журнал им. И.М.Сеченова**, 84(1-2): 133-138, 1998 (in Russian).
7. WU Y., CAZORLA O., LABEIT D., LABEIT S., GRANZIER H. Changes in titin and collagen underlie diastolic stiffness diversity of cardiac muscle. **J Mol Cell Cardiol**, 32: 2151-2161, 2000.
8. TSHOVREBOVA L., TRINICK J., SLEEP J.A. Elasticity and unfolding of single molecules of the giant muscle protein titin. **Nature**, 387(5): 308-312, 1997.
9. DECRAEMER W.F., MAES M.A., VANHUYSE V.J. An elastic stress-strain relation for soft biological tissue based on a structural model. **J of Biomech**, 13: 463-568, 1980.
10. DECRAEMER W.F., MAES M.A., VANHUYSE V.J., VANPEPERSTRAETE P. A non-linear viscoelastic constitutive equation for soft biological tissue based upon a structural model. **J of Biomech**, 13: 559-564, 1980.

## **МОДЕЛИРОВАНИЕ СТАЦИОНАРНОЙ ХАРАКТЕРИСТИКИ СИЛА-ДЕФОРМАЦИЯ ДЛЯ ПАССИВНОГО МИОКАРДА**

**Ю.Л. Проценко, А.В. Кобелев, Р.М. Кобелева, С.М. Руткевич  
(Екатеринбург, Россия)**

Исследованы упругие свойства изолированного препарата миокарда в стационарном состоянии в изометрическом режиме при редкой частоте стимуляции, в промежутках между одиночными сокращениями. Методикой, изложенной ранее, проведены измерения напряжения и поперечного размера при изменении длины образца на папиллярной мышце кролика. Обнаружена нелинейность зависимости «напряжение-деформация», выраженная в «ужесточении» образца при увеличении его длины, и установлена связь величины поперечного и продольного размеров препарата миокарда при деформации. Предложено математическое описание в рамках двумерной структурно-функциональной модели реологических свойств неоднородного миокарда. Модель содержит линейные гуксовские элементы и описывает нелинейный характер упругих свойств миокарда благодаря изменению ее геометрии при растяжении. Рассмотрено девять топологически различных типов таких моделей и получены зависимости «деформация-напряжение» для каждой из них. При аппроксимации экспериментальных данных для двух моделей оценены значения геометрических размеров и коэффициентов жесткости составляющих гуксовских элементов. Библ. 10.

Ключевые слова: биомеханика сердечной мышцы, кривые «напряжение-деформация», нелинейность механических свойств

*Received 15 August 2001*